



# MIT Open Access Articles

## *Mag-Foot: a steel bridge inspection robot*

The MIT Faculty has made this article openly available. **Please share** how this access benefits you. Your story matters.

<b>Citation</b>	Mazumdar, A., and H.H. Asada. "Mag-Foot: A steel bridge inspection robot." Intelligent Robots and Systems, 2009. IROS 2009. IEEE/RSJ International Conference on. 2009. 1691-1696. ©2009 IEEE.
<b>As Published</b>	<a href="http://dx.doi.org/10.1109/IROS.2009.5354599">http://dx.doi.org/10.1109/IROS.2009.5354599</a>
<b>Publisher</b>	Institute of Electrical and Electronics Engineers
<b>Version</b>	Final published version
<b>Accessed</b>	Sun Feb 01 08:22:01 EST 2015
<b>Citable Link</b>	<a href="http://hdl.handle.net/1721.1/60273">http://hdl.handle.net/1721.1/60273</a>
<b>Terms of Use</b>	Article is made available in accordance with the publisher's policy and may be subject to US copyright law. Please refer to the publisher's site for terms of use.
<b>Detailed Terms</b>	

# Mag-Foot: A Steel Bridge Inspection Robot

Anirban Mazumdar, H. Harry Asada, *Member, IEEE*

**Abstract**— A legged robot that moves across a steel structure is developed for steel bridge inspection. Powerful permanent magnets imbedded in each foot allow the robot to hang from a steel ceiling powerlessly. Although the magnets are passive, the attractive force is modulated by tilting the foot against the steel surface. This allows the robot to slide its feet along the surface using “Moonwalk” and “Shuffle” gait patterns. The robot can also detach its feet and swing them over small obstacles. These diverse walking patterns are created with a single servoed joint and 2 sets of simple locking mechanisms. Kinematic and static conditions are obtained for the under-actuated legged robot to perform each gait pattern safely and stably. A proof-of-concept prototype robot is designed, built, and tested. Experiments demonstrate the feasibility of the design concept and verify the analytical results.

**Index Terms**—Field robotics, underactuated systems, optimal control.

## I. INTRODUCTION

As the civil infrastructure of the world ages, time begins to take its toll on these structures in the form of corrosion and cracks. Undetected corrosion and cracks can severely compromise the structure and can lead to catastrophic failures that cannot be predicted. There exist more than 130,000 steel bridges in the United States alone [1].

In the absence of imbedded monitoring systems developed recently, these old bridges must be inspected periodically. Currently, many bridges are simply inspected visually by workers using temporary scaffolding or other means to reach the underside of bridges. Not only are such inspections time consuming, difficult, and at times dangerous, but published reports indicate that factors such as traffic, visual acuity, and accessibility may create variability in the ratings provided by human inspectors [2].

Due to these reasons described above, periodic bridge member inspection is a task where the current advances in mobile robots and robotic technology can be applied. A

bridge inspection robot has recently been presented [3] which uses a robotic device mounted on a custom road vehicle to take measurements. Another approach is to use mobile robots that can either grab the steel members or adhere using vacuum forces [4].

While these robots are valuable for performing periodic inspections, they cannot match the long term, continuous measurements that the modern imbedded sensor systems can provide. Specifically, imbedded sensor systems provide data in real time, provide data from multiple locations simultaneously, and provide data while the bridge is subjected to full loads and traffic [5],[6].

What we propose is to create a new inspection methodology that uses multiple small mobile robots to create a virtual sensor network that can be used on existing steel bridges. Such robots would “live” on their target bridges and would provide real time visual and acceleration measurements. Multiple robots could provide readings from multiple points (in order to measure vibration dynamics). In addition, unlike imbedded sensors, the robots would be able to change their locations on the bridge in order to provide a comprehensive map of the structure.

While there will be locations on the bridges that are inaccessible to the robots, there currently exists substantial research in estimating the presence of bridge damage from measurements of the frequency response and mode shapes of the structure [7]. These estimation methods could provide an early indication of potential damage that could be followed by more thorough inspections [8].

Since the robot is designed to act as a mobile sensor that “lives” on the bridge structure, reducing power consumption is extremely important. In this paper an alternative approach to bridge inspection mobile robots will be presented. Permanent magnets are used for adhering to steel structures, which consume no battery power. Magnets are imbedded in specially designed feet which use multiple gait patterns to flexibly negotiate irregular steel surfaces. Despite this variety of gait patterns, the robot employs only one servoed joint and two sets of locking mechanisms allowing the robot to remain lightweight and minimize power consumption. In the following, functional requirements for such bridge inspection robots will be described, followed by the low power Mag-Foot robot design. Kinematic and static properties of various gait patterns will be analyzed and a prototype robot is designed, built, and tested at the end.

Manuscript received August 1, 2009.

A Mazumdar is with the Department of Mechanical Engineering at the MIT, Cambridge, MA 02139 (phone: 617-258-0811, email: amazumda@mit.edu).

H. Harry Asada is a professor with the Department of Mechanical Engineering at MIT, Cambridge, MA 02139 (email: asada@mit.edu).



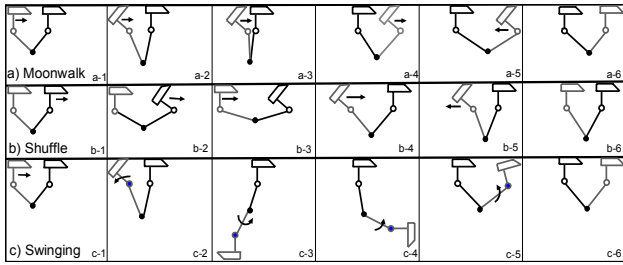


Fig. 4. An illustration of the 3 gait modes. Idealized time sequences for the Moonwalk (a), the Shuffle (b), and Swinging (c) are provided. The arrows illustrate the direction of motion that occurs between the current frame and the next frame.

Foot 2 slides past Foot 1 (a-4), the foot is stopped at an appropriate distance (a-5). Finally a positive torque is used to rotate Foot 1 backwards so that it can fully engage with the steel surface. The process is repeated as gait proceeds.

Note that, when Foot 2 passes Foot 1, joints A and C momentarily come to the same location. As will be discussed later in detail, an undesired behavior may occur at this particular configuration, since legs 1 and 2 together can freely rotate about joint A (C). It is a type of singularity.

To prevent this singularity configuration from occurring, we use another gait mode, called the “Shuffle.” First, a positive torque is applied at the hip joint to tilt Foot 1 (b-2) and push Foot 1 forward. With a negative torque at joint B, the tilted Foot 1 returns to the planted configuration and Foot 2 begins to tilt (b-4). After pulling Foot 2 forward (b-5), the hip joint pushes Foot 2 back to the surface (b-6), and repeats the process.

The third gait mode is called “Swinging.” First, a negative torque is used to tilt Foot 2 (c-2). Once the foot is tilted, ankle joint C is locked. Now that the magnetic force at Foot 2 has been reduced, a positive torque is used to pull Foot 1 off the surface (c-3). The foot is then swung around and the process is repeated.

#### IV. KINEMATIC AND STATIC ANALYSIS

##### A. Kinematic Analysis

The three gait modes described above consist of a few motion primitives. Figs. 5-7 show the equivalent kinematic models depicting each of the motion primitives.

1) *Foot Tilting*: One of the motion primitives is to tilt a foot by rotating it about point B in Fig.2. This foot tilting is required for all the three gait modes. As shown in Fig.5, the rotating foot, the two legs, and the fixture form a four-bar linkage. Let  $\beta$  be the angle of foot rotation about point B. There exists a functional relationship between the hip angle  $\theta$  and this foot rotation angle:

$$\beta = \beta(\theta) \quad (2)$$

This implies that the servoed joint angle,  $\theta$ , determines the foot tilting angle  $\beta$ . The detailed result can be found in [9].

2) *Foot Sliding*: Following the tilting motion, the foot must be moved along the surface. This sliding primitive, too, is

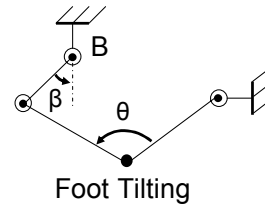


Fig. 5. A diagram illustrating the tilting primitive.

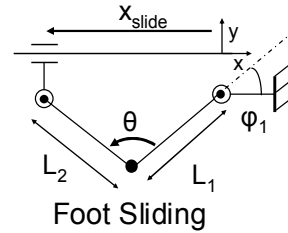


Fig. 6. A diagram illustrating the sliding primitive.

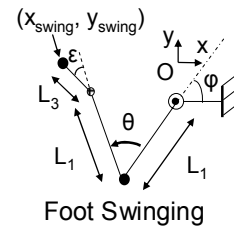


Fig. 7. A diagram illustrating the swinging primitive.

involved in all three gait modes. We assume that the angled toe surface is completely aligned to the surface making a surface-to-surface contact. Under this assumption, the foot sliding can be modeled as another four-bar-linkage with one prismatic joint along the surface and three revolute joints as shown in Fig. 6. If we recall that the leg length is  $L_i$  for both legs, the relationship between the distance between the legs,  $x_{slide}$ , and the hip angle,  $\theta$ , can be determined.

$$x_{slide} = -2L_1 \sin \frac{\theta}{2} \quad (3)$$

3) *Swinging*: The swinging mode introduces a new set of independent generalized coordinates for describing the kinematics. The rear foot is assumed to be locked at an angle  $\epsilon$ . The length of the leg and the foot are defined as  $L_1$  and  $L_2$  respectively. Now both the ankle angle,  $\phi$ , and the hip angle,  $\theta$ , are required to determine the position of the tilted foot ( $x_{swing}, y_{swing}$ ).

$$\begin{bmatrix} x_{swing} \\ y_{swing} \end{bmatrix} = \begin{bmatrix} -L_1 \cos \phi + L_1 \cos(\phi + \theta) + L_3 \cos(\phi + \theta + \epsilon) \\ -L_1 \sin \phi + L_1 \sin(\phi + \theta) + L_3 \sin(\phi + \theta + \epsilon) \end{bmatrix} \quad (4)$$

##### B. Singularity Analysis

Kinematic analysis reveals the presence of a type of singularity at  $\theta = 0$  for the sliding mode. We can use the analysis used in [11], by beginning with a generalized linkage shown in Fig. 6.

$$\sin \theta = \frac{L_2}{L_1} \cos \phi_1 \sin \phi_1 \pm \sin \phi_1 \sqrt{1 - \left(\frac{L_2}{L_1}\right)^2 \sin^2 \phi_1} \quad (5)$$

Since during the sliding mode, Leg 1 and Leg 2 are of equal

length ( $L_1$ ), the relationship exists between the ankle joint value angle ( $\varphi_1$ ) and the hip angle ( $\theta$ ) simplifies.

$$\sin \theta = \sin \phi_1 \cos \phi_2 \pm \sin \phi_1 \cos \phi_1 \quad (6)$$

$$\sin \theta = \begin{cases} \sin \phi_1 \cos \phi_1 \\ 0 \end{cases} \quad (7)$$

Therefore the kinematic relationship between  $\varphi_1$  and  $\theta$  breaks down at  $\sin \theta = 0$  indicating the presence of a kind of singularity [11]. At this configuration, the ankle angles,  $\varphi_1$  and  $\varphi_2$ , are independent of  $\theta$  and are therefore no longer defined by the mechanism.

This is especially problematic in light of the fact that the Mag-Foot robot is intended to walk on inclined surfaces. Gravity can act on the mechanism and cause its configuration to change. This problem necessitated the development of the ‘‘Shuffle’’ gait mode described in section IV. This gait allows the Mag-Foot robot to walk along surfaces without passing through the singularity.

### C. Static Analysis

In the above kinematic analysis using the equivalent kinematic models we assumed that all revolute and prismatic joints do not disjoint. In reality, magnetic feet may be detached from the surface, since they are held by magnetic forces, not by structures. We have to assure that at least one foot remains completely fixed while the other moves. Should this ‘‘planted’’ foot fail to remain fixed, the robot is likely to fall. For the other foot, too, it must not lose contact with the surface while it is rotating or sliding. Furthermore, to perform the swinging mode gait one foot must be secured while the other must be detached from the surface in the face of the adhesive magnetic force.

1) *Tilting*: The foot must tilt before sliding. Performing simple static analysis on the robot mechanism provides the motor torque,  $\tau_{\text{tilt}}$ , requirements for making the foot tilt before sliding. Let  $m_B$  be the total mass of the hip assembly,  $\mu_{s,i}$  the static coefficient of friction between Foot  $i$  (either 1 or 2) and the surface, and  $F_m(d)$  represents the magnetic clamping force as a function of the air gap  $d$ . Also recall that  $r$  represents the distance from the center of the magnet to the tilting edge of the foot, and  $w$  represents the  $x$  distance from the rear edge to the center of the magnet. The torque needed for tilting the foot is given.

$$\tau_{\text{tilt}} = \frac{L_1 \left( F_m(0)r - \frac{m_B g}{2} \left( (w+r) + h \tan \frac{\theta}{2} \right) \right)}{(w+r) \sin \frac{\theta}{2} - h \cos \frac{\theta}{2}} \quad (8)$$

Note that the worst case scenario is  $d = 0$  (no air gap means highest magnetic force) therefore, this will be used for determining actuator specifications.

The above analysis can be used in combination with basic static analysis on the mechanism to determine at which configurations the mechanism will fail. The goal is to determine at what configurations the planted foot will no

longer remain planted. Foot 1 will detach when the following condition is violated.

$$F_y^1 < -F_m(0) \quad (9)$$

Note that the distance  $d$  is set to zero because Foot 1 is assumed to be planted. The results of this static analysis are provided in Fig. 8. Fig. 8 plots the normalized hip torque versus the hip angle. A number of values for the mass  $m_B$  are provided, illustrating how changing the mass can alter the torque requirements substantially.

The cross hatched areas in Fig. 8 show the limits to  $\theta$  due to the conditions (9). This result provides important insights into the design because it illustrates that tilting cannot occur at certain configurations that therefore must be avoided.

The ‘‘tilt before sliding’’ is based on the existence of a friction force between the foot and the surface. If the surfaces in question are slippery and do not provide sufficient friction, problems can arise. For example if the conditions (10) are violated at Foot 2, the foot will tend to slide forwards rather than tilting. Similarly, if the condition is violated for Foot 1, the planted foot will slide backwards.

$$\mu_{s,i} > \frac{r}{h} \quad (10)$$

Since sliding instead of tilting is problematic, it would be advisable to design the feet with rough features so that the friction coefficient is maximized. Nevertheless there will likely be conditions (such as ice) under which the robot cannot operate.

2) *Sliding*: Similarly, static analysis can be used to determine the sliding torque  $\tau_{\text{slide}}$ . A key assumption here is that the foot tilts completely so that the angled toe surface is now parallel with the steel surface. This is essential for the sliding mode kinematics. Using the same assumptions as those outlined above, the torque necessary to slide the foot from rest along a surface with static friction coefficient  $\mu_s$  can be computed. Note that the normal force between the foot and the surface is again approximated as  $F_m(d)$  (the clamping force of the magnet). The result is provided (11).

$$\tau_{\text{slide}} = L_1 \left( \frac{m_B g}{2} \sin \frac{\theta}{2} - F_m(d_{\text{slide}}) \frac{r}{h} \cos \frac{\theta}{2} \right) \quad (11)$$

Note that the air gap  $d$  is now set to  $d_{\text{slide}}$ . Since  $d_{\text{slide}}$  is greater than zero, the torque contribution from the magnetic force is reduced substantially. A negative torque causes the foot to slide in the positive  $x$  direction. This is a result of the use of a right handed coordinate system.

4) *Foot Detachment for Swinging*: The torque necessary to detach the foot from the surface must be considered. For detachment, the ankle joint must be locked so the angle between Foot 2 and the leg is fixed.

Following an approach similar to that for the tilting case, free body diagrams were used to determine the forces on the mechanism as a result of the detachment torque. Since the locked angle,  $\varepsilon$ , is small the kinematics can be simplified. The estimate for the detachment torque is provided (12). The air

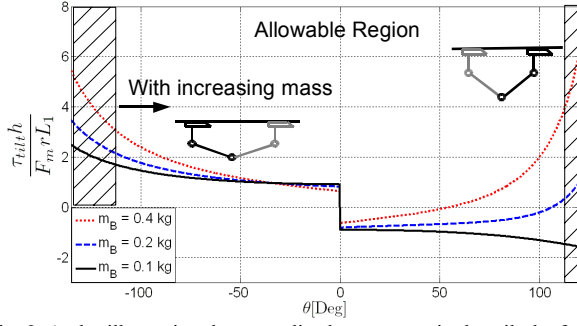


Fig. 8. A plot illustrating the normalized torque required to tilt the foot based on the hip angle,  $\theta$ , for different hip mass  $m_B$  values.

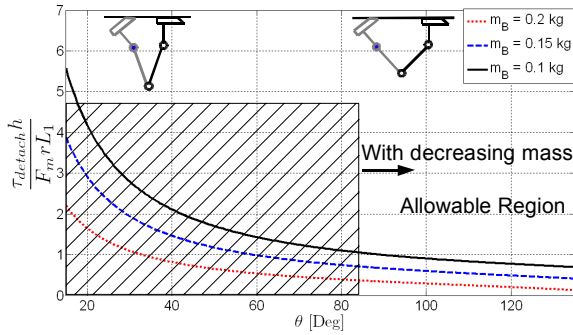


Fig. 9. A plot illustrating the normalized torque required to detach the foot based on the hip angle,  $\theta$ .

gap  $d$  is set to  $d_{lock}$ , where  $d_{lock}$  is greater than zero. This means that the magnetic force  $F_m(d)$  is small.

$$\tau_{detach} = \frac{(L_1 + L_2) \left( F_m(d_{lock}) - \frac{m_B g}{2} \right)}{\sin \frac{\theta}{2}} \quad (12)$$

Note that the detachment torque can potentially cause Foot 2 to either tilt or detach. The tendency to tilt is especially dangerous because the tilting foot is designed so that it will tilt with a low horizontal force  $F_x^A$ .

The results of this static analysis are provided in Fig. 9 which plots the required detachment torque,  $\tau_{detach}$  versus hip angle  $\theta$ . The cross hatched sections are used to provide an illustration of the working range of the robot.

## V. IMPLEMENTATION

### A. Robotic System

A Mag-Foot robot prototype was designed, analyzed and constructed. It is essentially a planar mechanism, but uses a 3-feet arrangement to resist moments about the y axis. As Fig. 10 illustrates, an inner foot lies between two outer feet which move together. The hip actuator is a Pololu 67:1 20Dx45L mm metal 6V DC planetary gearmotor (1260°/s no load speed, 0.402 N-m stall torque).

The locking action at the ankles for the swinging motions

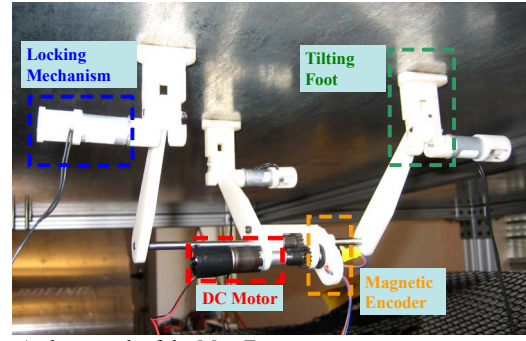


Fig. 10. A photograph of the Mag-Foot prototype

was provided by small solenoid actuators. The mechanism was designed so that rotation in one direction was allowed but while rotations in the other direction are prevented. This means that the foot will not rotate during detachment but can rotate in the other direction, allowing it to align itself for a limited set of landing configurations.

### B. Tilting Foot

6mm diameter, nickel plated, N38 magnets (attachment force  $\sim 4$ N) were used for the feet.

### C. Control

A National Instruments CompactRIO programmable automatic controller was used in tandem with custom written LabView control software for the logic and control of the robotic device. The real time control operated at a sampling rate of 2 kHz.

### D. Measurement

A 10 bit absolute magnetic shaft (US Digital, MAE3-A10-188-220-7-1) encoder was used to measure the hip angle.

### E. Sliding Primitive Control

The sliding mode gait is essentially a closed loop servo control problem. A Proportional + Derivative (PD) controller was used to control the hip angle for gait control.

### F. Swinging Primitive Control

The swing-up motions of this type of robot present a unique set of dynamics and controls challenges; the robot is underactuated and subject to certain force constraints imposed by the tilting foot design. This “swinging problem” is addressed in depth in [12].

## VI. RESULTS

### A. Moonwalk and Shuffle Results

To evaluate the Moonwalk, the Mag-Foot robot was allowed to hang on a flat steel surface. The robot was then commanded to take the two steps that comprise the gait. To test the Shuffle gait, the robot was commanded to walk along a flat steel surface inclined at 15°. The results of these two experiments are illustrated in Figs 11 and 12.

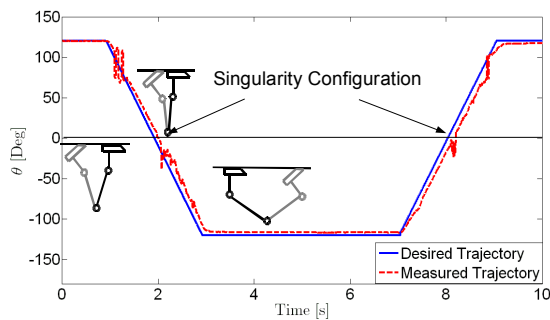


Fig. 11 A plot illustrating the closed loop control over the hip angle,  $\theta$ , during the Moonwalk gait.

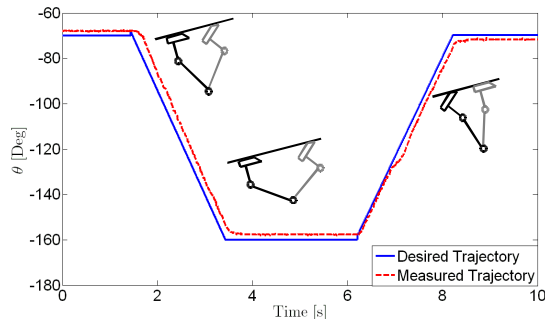


Fig. 12 A plot illustrating the closed loop control over the hip angle,  $\theta$ , during the Shuffle gait.

### B. Swinging Mode Results

To evaluate the swinging mode, the robot was allowed to hang on a flat steel surface and then commanded to perform the sequence of steps described in section III. Fig. 13 shows the frames of a video illustrating how one foot was tilted and locked (a), detached (b), and swung around (c), and allowed to land softly (d).

## VII. CONCLUSION

This work has described the design, analysis, and control of a new type of robot for the inspection of steel surfaces such as bridge members. We outlined a novel tilting foot design that allows us to modulate the force of permanent magnetic feet by introducing an air gap. We used this tilting foot to create a robotic device (titled “Mag-Foot”) capable of three unique modes of locomotion; the Moonwalk can be used for moving quickly along flat surfaces, the Shuffle can be used for walking along surfaces with small inclines, and the swing can be used to traverse small obstacles. The robot performs these actions while using only a single actuator in tandem with simple locking mechanisms.

Finally, we designed and constructed an initial prototype. Experimental studies were used to verify the validity of the design as well as the efficacy of the moonwalk and shuffle gait modes.

There exist limitations to the current design and implementation. First, the initial prototype is limited to a single plane of motion. We have proposed a new design to address this [9], but this design must be verified physically.

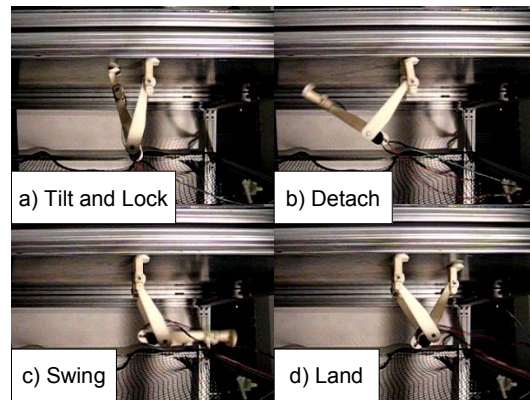


Fig. 13 A photograph illustrating the Swing gait.

In addition, the magnetic feet are dependent on friction to tilt before sliding. Therefore the tilting feet are unsuitable for highly slippery surfaces. Finally, this design is limited to walking upside down on relatively flat surfaces. While this may be sufficient for bridge surfaces, this limits the applicability of the design.

## REFERENCES

- [1] U.S. Department of Transportation Federal Highway Administration National Bridge Inventory Data. Available online at <http://www.fhwa.dot.gov/bridge/nbi.htm>
- [2] U.S. Department of Transportation, Federal Highway Administration. (2001). *Reliability of Visual Inspection for Highway Bridges, Volume I: Final Report*. (FHWA-RD-01-020).
- [3] J. Oh, A. Lee., S. Oh, Y. Choi, B. Yi, H.W. Yang, “Design and Control of Bridge Inspection Robot System”, *Proceedings of the IEEE International Conference on Mechatronics and Automation*, Harbin, China, pp. 3634-3639, Aug. 2007.
- [4] C. Balaguer, A. Gimenez, M. Abderrahim, “Climbing Robots for Inspection of Steel Based Infrastructures.” *Industrial Robot*, Vol. 29, no. 3. pp. 246-251, 2002.
- [5] C-Y. Kim, D-S Jung, N-S Kim, S-D. Kwon, M.Q. Feng, “Effect of Vehicle Weight on natural frequencies of bridges measured from traffic-induced vibration,” *Earthquake Engineering and Engineering Vibration*, Vol.2, no.1, pp 109-106, 2003.
- [6] E. Ntotsios, C. Padadimitriou, P. Panetsos, G. Karaiskos, K. Perros, P.C. Perdikaris, “Bridge Health Monitoring System based on Vibration Measurements,” *Bull Earthquake Eng*, Vol. 7, pp 469-483, 2009.
- [7] P.Cawley, R. D. Adams, “The Location of Defects in Structures from Measurements of Natural Frequencies,” *Journal of Strain Analysis*, Vol. 14, No. 2, pp 49-57.
- [8] D-S Hong, H-S Do, J-T Kim, W-B Na, H-M Cho, “Hybrid Vibration-Impedance Approaches for Damage Detection in Plate-Girder Bridges, Proc. Of SPIE, Vol. 6935: Health Monitoring of Structural and Biological Systems 2008.
- [9] A. Mazumdar, “Mag-Feet: A Robotic Device for the Inspection of Steel Bridge Structures,” SM Thesis, Department of Mechanical Engineering, Massachusetts Institute of Technology, Cambridge Massachusetts.
- [10] A. Slocum, S. Awtar, A. Hart, “Magnebots: A Magnetic Wheels Based Overhead Transportation Concept”, *Proceedings of the 2<sup>nd</sup> IFAC Mechatronics Conference*, Berkeley, CA, pp 833, Nov. 2002.
- [11] C. Gosselin, J. Angeles, “Singularity Analysis of Closed Kinematic Chains,” *IEEE Transactions on Robotics and Automation*, Vol 6, no. 3, pp. 281-290, 1990.
- [12] A. Mazumdar, H. Asada, “Optimal Control of a Magnetically Suspended Underactuated Robot for Swing-Up Motion,” To be printed in the Proceedings of the ASME Dynamic Systems and Controls Conference (DSCC), Hollywood California, 2009.